Electronic Supplementary Information

Cu(II) and V(VI)O complexes with tri- or tetradentate ligands based on (2-hydroxybenzyl)-L-alanines reveal promising anticancer therapeutic potential

Nádia Ribeiro[1$], Ipek Bulut[2$], Buse Cevatemre[3$], Carlos Teixeira[1$], Yasemin Yildizhan[4], Vânia André[1], Pedro Adão[5], João Costa Pessoa[1], Ceyda Acilan[2,3*], Isabel Correia[1*]

[1]*Centro de Química Estrutural and Departamento de Engenharia Química, Instituto Superior Técnico, Av. Rovisco Pais 1, 1049-001 Lisboa, Portugal*

[2]*Koç University, School of Medicine, Koç University, Sariyer, Turkey*

[3]*Koç University Research Center for Translational Medicine (KUTTAM), Sariyer 34450, Turkey*

[4]*TUBITAK, Marmara Research Center, Genetic Engineering and Biotechnology Institute, Kocaeli, Turkey*

[5]*MARE - Centro de Ciências do Mar e do Ambiente, Politécnico de Leiria, Edifício CETEMARES, Av. Porto de Pesca, 2520-630 Peniche, Portugal*

S1 – Synthesis and characterization of the compounds

S1.1. Ligand synthesis

Synthesis of H_2L^1-H_2L^4 - L-phenylalanine or L-valine, depending on the desired product, and NaOH (1.2 eq/mmol amino acid) were weighted and introduced in a round bottom flask equipped with a reflux condenser, and dissolved in MeOH (2.50 mL/mmol amino acid) at room temperature (RT). To the resulting colorless solution, paraformaldehyde (1.0 eq/mmol amino acid) was added to the mixture and allowed to stir for 1 h at RT. The disubstituted phenol (1.0 eq/mmol amino acid) was then added and the reaction was refluxed for 16 h; the heating was then stopped, and the reaction cooled to RT. Concentrated HCl was added dropwise till pH~6, affording a white precipitate. Distilled water was generously added to the mixture and the suspension filtered under vacuum and washed with 3x50 mL of distilled water and 1x50 mL petroleum ether, yielding the desired product.

(*S*)-2-[(2-hydroxy-3,5-dimethylbenzyl)ammonio]-3-phenylpropanoate (H_2L^1)

Reagents: L-Phenylalanine (3.30 g, 20.0 mmol), NaOH (0.96 g, 24.0 mmol), paraformaldehyde (0.60 g, 20.0 mmol), 2,4-dimethylphenol (2.42 mL, 20.0 mmol), MeOH (50 mL). The compound was obtained as an amorphous white solid. Yield: 64% (3.83 g). Elemental analysis for $C_{18}H_{21}NO_3$: Calcd. C 72.22, H 7.07, N 4.68; found C 72.1, H 7.2, N 4.7. ESI-MS m/z [Found % (Calcd)]: 300.02 100% (300.16) $[L+H]^+$. ν_{max}/cm^{-1}: 3149 (N-H, w), 1578 (C=$O_{carboxyl}$, w), 1231 (C-O_{Phenol}, w). δ_H (300 MHz, D_2O + Na_2CO_3 + Acetone-d_6, ppm) 7.39-7.12 (5H, m, Ar**H*Phenyl* 8**), 6.86 (1H, s, ArH*Phenol*, *para* to CH2NH2+ **7**), 6.68 (1H, s, ArH*Phenol*, *ortho* to CH2NH2+ **6**), 3.87 (1H, d, NH2+C**HH**PhOH, *J*= 13.9Hz **5A/B**), 3.53 (1H, d, NH2+C**HH**PhOH, *J*= 14.0Hz **5A/B**), 3.30 (1H, dd, PhCH2C**H**COO-, *J*= 8.4, 5.7Hz **4**), 2.98 (1H, dd, PhC**HH**CHCOO-, *J*= 13.7, 5.3Hz **3M**), 2.78 (1H, dd, PhC**HH**CHCOO-, *J*= 13.7, 8.4Hz **3A**), 2.11 (3H, s, ArC**H3**, *ortho* to HO*Phenol* **2**) 1.99 (3H, s, ArC**H3**, *para* to HO*Phenol* **1**). δ*C* (75.4 MHz, D2O + Na2CO3 + Acetone-*d*6, ppm): 181.30 (1C, **C**OO-), 153.59 (1C, **C*ipso,Phenol***), 138.83 (1C, **C*ipso,Phenyl***), 130.56 (1C, Ar**C**H***Phenol***, *para* to CH2NH2+), 129.41 (2C, Ar**C**H***Phenyl***, *ortho* to CH2), 128.84 (2C, Ar**C**H***Phenyl***, *meta* to CH2), 128.46 (1C, Ar**C**CH3, *ortho* to HO*Phenol*), 127.23 (1C, Ar**C**H***Phenol***, *ortho* to CH2NH2+), 126.90 (1C, Ar**C**H***Phenyl***, *para* to CH2),

125.63 (1C, Ar**C**CH3, *para* to HO*Phenol*), 123.68 (1C, Ar**C**OH*Phenol*), 64.22 (1C, -OOC**C**HCH2Ph), 49.65 (1C, NH2+**C**H2PhOH), 39.19 (1C, -OOCCH**C**H2Ph), 19.61 (1C, Ar**C**H3, *ortho* to HO*Phenol*), 15.27 (1C, Ar**C**H3, *para* to HO*Phenol*).

(*S*)-2-[(2-hydroxy-3,5-dimethylbenzyl)ammonio]-3-methylbutanoate (H_2L^2)

Reagents: L-Valine (2.35 g, 20.0 mmol), NaOH (0.96 g, 24.0 mmol), paraformaldehyde (0.60 g, 20.0 mmol), 2,4-dimethylphenol (2.42 mL, 20.0 mmol), MeOH (50 mL). The compound was obtained as a white solid. Yield: 49% (2.45 g). Elemental analysis for $C_{14}H_{21}NO_3$: Calcd. C 66.91, H 8.42, N 5.57; found C 66.7, H 8.0, N 5.4. ESI-MS m/z [Found % (Calcd)]: 253.03 65% (252.16) $[L+H]^+$. ν_{max}/cm^{-1}: 2964 (N-H, s, b), 1564 ($C{=}O_{carboxyl}$, s), 1229 ($C\text{-}O_{Phenol}$, s). δ_H (300 MHz, CD_3OD, ppm): 6.98 (1H, s, Ar**H**, *para* to CH2NH2+), 6.93 (1H, s, Ar**H**, *ortho* to CH2NH2+), 4.17 (2H, dd, NH2+C**H2**PhOH, *J*= 29.6, 12.9Hz), 3.38 (1H, d, NH2+C**H**COO-, *J*= 3.8Hz), 2.30-2.20 (1H, m, C**H**(CH3)2, partially overlapped with ArCH3), 2.22 (6H, s, respective to all ArC**H3**), 1.05, 1.02 (3H each, d each, CH(C**H3**)2, partially overlapped, *J*= 7.1 and 7.0Hz respectively). δ*C* (75.4 MHz, CD3OD, ppm): 172.46 (1C, **C**OO-), 153.05 (1C, Ar**C**OH), 134.12 (1C, Ar**C**H, *para* to CH2NH2+), 130.76 (1C, ArC**C**H3, *para* to HO*Phenol*), 130.56 (1C, Ar**C**H, *ortho* to CH2NH2+), 126.17 (1C, ArC**C**H3, *ortho* to HO*Phenol*), 119.41 (1C, ***Cipso,Phenol***), 68.46 (1C, NH2+**C**HCOO-), 49.40 (1C, NH2+**C**H2PhOH), 30.60 (1C, **C**H(CH3)2), 20.39 (1C, Ar**C**H3, *ortho* to HO*Phenol*), 18.80, 18.62 (1C each, CH(**C**H3)2), 16.43 (1C, Ar**C**H3, *para* to HO*Phenol*).

(*S*)-2-[(3,5-di-*tert*-butyl-2-hydroxybenzyl)ammonio]-3-phenylpropanoate (H_2L^3)

Reagents: L-Phenylalanine (1.65 g, 10.0 mmol), NaOH (0.48 g, 12.0 mmol), paraformaldehyde (0.30 g, 10.0 mmol), 2,4-di-*tert*-buthylphenol (2.06 g, 10.0 mmol), MeOH (25 mL). The compound was obtained as a white solid. Yield: 66% (2.54 g). Elemental analysis for $C_{24}H_{33}NO_3.0.5H_2O$: Calcd. C 73.44, H 8.73, N 3.57; found C 73.1, H 8.8, N 3.3. ESI-MS m/z [Found % (Calcd)]: 384.09 100% (384.26) $[L+H]^+$. ν_{max}/cm^{-1}: 2955 (N-H, m), 1733 ($C{=}O_{carboxyl}$, w), 1227 ($C\text{-}O_{Phenol}$, m). δ_H (300 MHz, CD_3OD, ppm): 7.40-7.25 (6H, m, Ar**H**), 7.04 (1H, s, Ar**H***Phenol*, *para* to CH2NH2+), 4.15, 3.97 (1H each, d each, NH2+C**H2**PhOH, *J*= 13.0Hz each), 3.84 (1H, dd,

NH2+C**H**CH2Ph, *J*= 8.5, 5.0Hz), 3.35 (1H, dd, NH2+CHC**HH**Ph, partially overlapped with CD3OD signal, *J*= 14.5, 8.6Hz), 3.07 (1H, dd, NH2+CHC**HH**Ph, *J*= 14.5, 8.6Hz) 1.39 (9H, s, C(C**H3**)3*, ortho* with HO*Phenol*), 1.27 (9H, s, C(C**H3**)3*, para* to HO*Phenol*). δ*C* (75.4 MHz, CD3OD, ppm): 173.39 (1C, **C**OO-), 153.87 (1C, $\mathbf{C}_{ipso,Phenol}$), 143.98 (1C, C_{Phenol}, *para* to HO*Phenol*), 139.65 (1C, $\mathbf{C}_{Phenol}$, *ortho* to HO*Phenol*), 137.34 (1C, $\mathbf{C}_{ipso,Phenyl}$), 130.42, 130.00 (2C each, Ar**C**H***Phenyl***, *ortho* and *meta* to CH2), 128.44 (1C, Ar**C**H, *para* to CH2), 127.00 (1C, Ar**C**H*Phenol*, *para* to CH2NH2+), 126.35 (1C, Ar**C**H*Phenol*, *ortho* to CH2NH2+), 121.22 (1C, Ar**C**OH), 64.28 (1C, NH2+**C**HCH2Ph), 49.61 (1C, NH2+**C**H2PhOH), 37.88 (1C, NH2+CH**C**H2Ph), 35.98 (1C, **C**(CH3)3*, ortho* to HO*Phenol*), 35.15 (1C, **C**(CH3)3*, para* to HO*Phenol*), 31.93 (3C, C(**C**H3)3*, para* to HO*Phenol*), 30.33 (3C, C(**C**H3)3*, ortho* with HO*Phenol*).

(*S*)-2-[(3,5-di-*tert*-butyl-2-hydroxybenzyl)ammonio]-3-methylbutanoate (H_2L^4)

Reagents: L-Valine (1.18 g, 10.0 mmol), NaOH (0.48 g, 12.0 mmol), paraformaldehyde (0.30 g, 10.0 mmol), 2,4-di-*tert*-buthylphenol (2.06 g, 10.0 mmol), MeOH (25 mL). The compound was obtained as a white solid. Yield: 61% (2.57 g). Elemental analysis for $C_{20}H_{33}NO_3$.0.5MeOH: Calcd. C 70.05, H 10.04, N 3.98; found 70.16, H 10.33, N 3.87. ESI-MS m/z [Found % (Calcd)]: 359.28 20% (358.24) $[L+Na]^+$: 336.08 15% (336.27) $[L+H]^+$. ν_{max}/cm^{-1}: 2956 (N-H, s), 1622 ($C=O_{carboxyl}$, m), 1203 ($C\text{-}O_{Phenol}$, m). δ_H (300 MHz, CD_3OD, ppm): 7.33 (1H, s, Ar**H**, *para* to CH2NH2+), 7.14 (1H, s, Ar**H**, *ortho* to CH2NH2+), 4.19, 4.01 (1H each, d each, NH2+C**H2**PhOH, *J*= 13.2Hz each), 3.31 (1H, m, HOOCC**H**CH(CH3)2, totally overlapped by CD3OD signal, determined by HSQC), 2.18 (1H, m, HOOCCHC**H**(CH3)2), 1.42 (9H, s, ArC(C**H3**)3, *ortho* to HO*Phenol*) 1.29 (9H, s, ArC(C**H3**)3, *para* to HO*Phenol*), 1.06, 1.03 (3H each, d each, CH(C**H3**)2, partially overlapped, *J*= 9.8Hz each). δ*C* (75.4 MHz, CD3OD, ppm): 174.41 (1C, **C**OO-), 154.30 (1C, Ar**C**OH), 143.64 (1C, Ar**C**(tButyl), *para* to HO*Phenol*), 139.16 (1C Ar**C**(tButyl), *ortho* to HO*Phenol*), 126.73 (1C, Ar**C**H, *ortho* to CH2NH2+), 125.83 (1C, Ar**C**H, *para* to CH2NH2+), 121.86 (1C, **C*ipso,Phenol***), 69.15 (1C, NH2+**C**HCH(CH3)2), 50.79 (1C, NH2+**C**H2PhOH), 35.98 (1C, **C**(CH3)3, *ortho* to HO*Phenol*), 35.16 (1C, **C**(CH3)3, *para* to HO*Phenol*), 31.99 (3C, C(**C**H3)3, *para* to

HO*Phenol*), 31.24 (1C, NH2+CH**C**H(CH3)2), 30.33 (3C, C(**C**H3)3, *ortho* to HO*Phenol*), 19.15 (2C, NH2+CHCH(**C**H3)2).

H_2L^5 - The synthesis and characterization of this ligand precursor were previously reported.[1]

H_2L^6 - The synthesis and characterization of this ligand precursor were previously reported.[1]

S1.2 Characterization

The synthetic pathway used in the preparation of H_2L^1-H_2L^4 was a Mannich reaction.[2] The amino acid sources, L-Phe or L-Val, were mixed with paraformaldehyde in methanol and the selected phenol was added to the mixture. The reduced Schiff bases were isolated in moderate yields in their zwitterionic forms. The amino acid-pyridyl-phenol ligand precursors H_2L^5-H_2L^6**,** also depicted in **Figure 1,** were successfully synthesized by a stepwise reductive alkylation – Mannich reaction procedure. Their synthesis and characterization was previously reported.[1]

The ^{1}H NMR spectrum of H_2L^1 is presented in **Figure S1**. It shows *C1*-symmetry in solution, consistent with the non-symmetric structure of the compound and with the existence of magnetically non-equivalent protons. The ^{1}H NMR spectra of H_2L^1 – H_2L^4 display a doublet of doublet AB system corresponding to the methylene bridging the amino group and the phenol moiety (**Fig. S1,** signal 5). A doublet of doublet three-spin AMX system is also evident in amino acid-phenol compounds derived from L-Phe, corresponding to coupling between the side-chain amino acid methylene and CH groups (signals 3 and 4 for H_2L^1).

FTIR spectroscopy afforded additional structural information with N-H and C=O stretching bands being detected around 3400-2900 and 1600 cm^{-1}, respectively. Phenolic C-O stretching bands were observed around 1200 cm^{-1} for the H_2L^1-H_2L^4 ligand precursors. Information provided by ESI-MS and elemental analyses (EA) support the expected molecular formulas for the prepared ligand precursors, as peaks corresponding to $[L+H]^+$ species were found in the MS spectra of all of them. Solvent molecules were considered in the EA analyses due to the hygroscopic nature of these compounds.

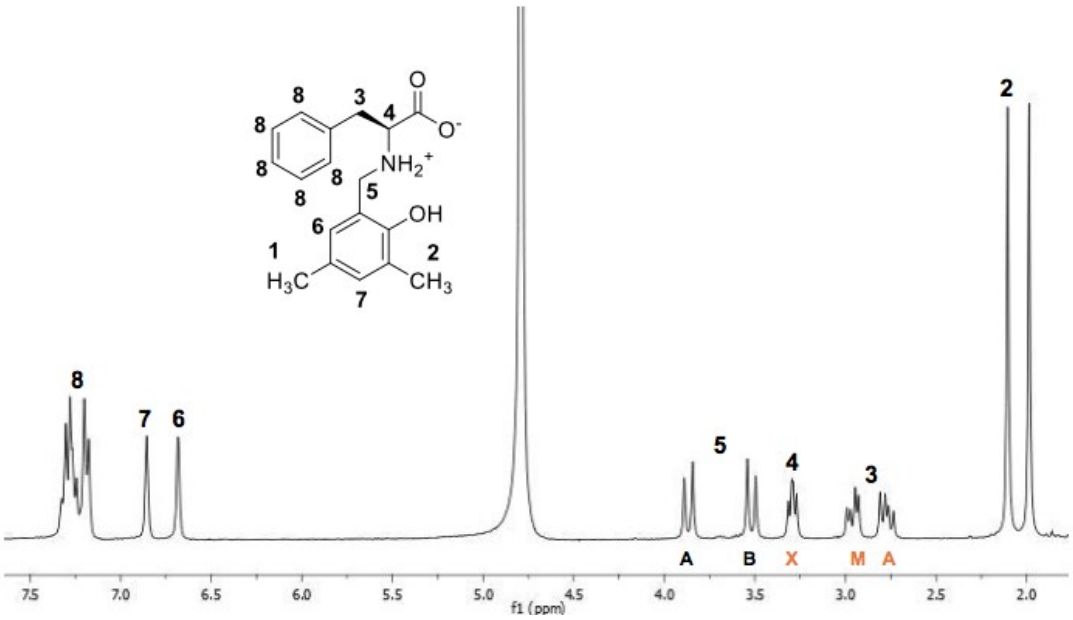

Figure S1 - ^{1}H NMR spectrum of H_2L^1 showing *C1*-symmetry in D_2O:Na_2CO_3 solution. The AMX doublet of doublet pattern is well resolved.

S1.3. The complexes

SC-XRD. From the slow evaporation of a H_2O/MeOH (*ca.* 5% v/v) solution of [Cu(HL^6)] (**9**) blue crystals were obtained and the structure was determined from SC-XRD data. The compound crystallized in the monoclinic *Cc* space group with two crystallographically independent copper complexes *per* asymmetric unit. Each Cu(II) center is five-coordinated by two O atoms and two N atoms of HL^6 and a chloride anion, forming a distorted square pyramidal coordination geometry (**Fig. 3**). The electron density map suggests that the carboxylic acid moieties are deprotonated coordinating to the metal center by one of the oxygen atoms, while the hydroxyl phenolic groups, for which the hydrogen atoms were located, coordinate in the axial position. The Cu-O_{OH} distances in the axial positions are slightly longer (Cu(1)-O(1) 2.373(6) Å and Cu(2)-O(4) 2.390(6) Å) than the basal distances (1.942(5)-2.224(3) Å for C(1) and 1.953(6)-2.217(2) Å for Cu(2)). The observed Cu-O_{OH} distances in [Cu(HL^6)] (**9)** are also consistent with those observed in structurally similar Cu(II) complexes bearing protonated phenol donor atoms.[3, 4] The distances of the Cu-axial ligand bond are in agreement with what is observed for related Jahn-Teller

distorted square-pyramidal Cu(II) complexes.[5, 6] The structural parameters (τ=0.067 and 0.072 for Cu(1) and Cu(2) respectively), which measure the degree of trigonality for five-coordinated structures (τ = 0 for a perfect square-based pyramid geometry and τ = 1 for perfectly trigonal-bipyramidal geometry),[7] confirm the square pyramidal geometry around the Cu(II) center. Selected bond lengths and angles are presented in **Table S1**.

Table S1. Bond lengths [Å] and angles [^{0}] for **9** as obtained from single crystal X-ray diffraction analysis.

Bond lengths [Å]		**Bond Angles [^{0}]**	
Cu(1)-O(2)	1.942(5)	O(2)-Cu(1)-N(2)	165.9(3)
Cu(1)-N(2)	2.006(7)	O(2)-Cu(1)-N(1)	83.0(3)
Cu(1)-N(1)	2.046(7)	N(2)-Cu(1)-N(1)	83.5(3)
Cu(1)-Cl(1)	2.224(3)	O(2)-Cu(1)-Cl(1)	94.1(2)
Cu(1)-O(1)	2.383(6)	N(2)-Cu(1)-Cl(1)	98.4(2)
Cu(2)-O(5)	1.953(6)	N(1)-Cu(1)-Cl(1)	169.9(2)
Cu(2)-N(4)	1.974(7)	O(2)-Cu(1)-O(1)	87.6(2)
Cu(2)-N(3)	2.034(7)	N(2)-Cu(1)-O(1)	96.7(2)
Cu(2)-Cl(2)	2.217(2)	N(1)-Cu(1)-O(1)	90.6(2)
Cu(2)-O(4)	2.390(6)	Cl(1)-Cu(1)-O(1)	98.93(17)
		O(5)-Cu(2)-N(4)	166.7(3)
		O(5)-Cu(2)-N(3)	83.6(3)
		N(4)-Cu(2)-N(3)	83.2(3)
		O(5)-Cu(2)-Cl(2)	96.2(2)
		N(4)-Cu(2)-Cl(2)	95.7(2)
		N(3)-Cu(2)-Cl(2)	162.4(2)
		O(5)-Cu(2)-O(4)	90.1(2)
		N(4)-Cu(2)-O(4)	91.9(3)
		N(3)-Cu(2)-O(4)	89.9(2)
		Cl(2)-Cu(2)-O(4)	107.68(16)

ESI-MS. Table S2 (and the Experimental section) list selected peaks found in electrospray ionization mass spectrometry (ESI-MS) spectra of the compounds and their assignment. For the vanadium complexes only peaks corresponding to oxidized species (V^V) were found. For complexes [VO(L^1)] (**1**) and [VO(L^2)] (**2**)**,** for which dinuclear species are a possibility in the solid state, only ionic species corresponding to monomeric V^VOL_2 (positive and negative) species were found, which further corroborates the monomeric formulation proposed. These are also found in the mass spectra of [VO(L^3)] (**3**) and [VO(L^4)] (**4**) as well as V^VOL type species (for **3**) and $(V^VOL)_2$. It was previously shown for an analogue of [VO(L^6)] (**5**) that oxidation takes place very fast in solution,[1] which is in agreement with the ESI-MS peaks found. Cu(II)-complexes lose the water molecule and the chloride anion upon ionization and form different types of ions, most of them of the CuL type, but also $(CuL)_2$.

Table S2 – Major species found in the spectra ESI-MS spectra (positive and negative modes) of methanolic solutions of the complexes.

Complex	ML species	ML_2 species	$(ML)_2$
VO(L^1) 1		$[V^VOL_2+H]^+$ (70) $[V^VOL_2-H]^-$ (100)	
VO(L^2) 2		$[V^VOL_2-H]^-$ (70) $[V^VOL_2+H]^+$(100)	
VO(L^3) 3	$[V^VOL+CH_3OH]^+$ (25)	$[V^VOL_2+H]^+$ (15)	$[(V^VOL+CH_3OH)_2+Na]^+$ (15)
VO(L^4) 4		$[V^VOL_2-H]^-$(100)	$[(V^VO_2L+CH_3OH)_2+K]^+$ (100)
VO(L^6) 5	$[V^VOL+CH_3O-H]^-$(100) $[V^VOL+CH_3O+H]^+$ (85) $[V^VOL+CH_3O+Na]^+$ (100)		
Cu(L^1) 6	$[CuL+H]^+$ (100)		$[(CuL)_2+H]^+$ (35)
Cu(L^3) 7	$[CuL+FA-H]^-$ (100) $[CuL+Cl]^-$ (20) $[CuL+ H]^+$ (25) $[CuL+CH_3OH+H+Na]^{2+}$ (100)		
Cu(HL^5) 8	$[CuL+H]^+$ (100) $[CuL+CH_3OH+H]^+$ (20)		$[(CuL)_2+K]^+$ (65)

Cu(HL^6) 9	$[CuL+Cl]^-$ (100) $[CuL+H]^+$ (100)

FTIR. The IR spectral data of complexes **1**–**9** are listed in **Table S3**, as well as for the ligand precursors. All complexes show a broad band centered at *ca.* 3400 cm^{-1} assigned to ν(O-H) of the coordinated (**5**-**9**) or uncoordinated water and/or methanol molecules, present in the compounds, which were also confirmed by EA. For the ligand precursors the antisymmetric $\nu_{as}(COO^-)$ and symmetric $\nu_s(COO^-)$ vibrations of the carboxylato moiety from the amino acid derivatives are in the range 1627 -1650 cm^{-1} and 1475-1487 cm^{-1}, respectively, while for the complexes they appear at 1538–1601 cm^{-1} and 1467–1488 cm^{-1}, respectively. The differences found between $\nu_{as}(COO^-)$ and $\nu_s(COO^-)$ are in agreement with monodentate coordination of this group.[8] The $\nu(C\text{-}O)_{phenol}$ is found in the usual range, between 1214-1244 cm^{-1}.[9] The strong and characteristic ν(V=O) bands appear at *ca.* 950-980 cm^{-1}, supporting the presence of mono-oxidovanadium(IV) complexes.[10, 11]

Table S3 – Selected FTIR bands (in cm^{-1}) and tentative assignments.

Compound	**ν(N-H)**	**$\nu_{as}(COO^-)$**	**$\nu_s(COO^-)$**	**$\nu(C\text{-}O)_{Phenol}$**	**ν(V=O)**
H_2L^1	3143	1594	1482	1232	-
$[VO(L^1)]$ **1**	3242	1628	1472	1226	963
$[Cu(L^1)]$ **6**	3242	1628	1474	1241	-
H_2L^2	3163	1620	1487	1226	-
$[VO(L^2)]$ **2**	3168	1640	1469	1214	975
H_2L^3	3242	1614	1475	1226	-
$[VO(L^3)]$ **3**	3244	1650	1467	1234	982
$[Cu(L^3)]$ **7**	3244	1627	1470	1232	-
H_2L^4	3272	1621	1480	1221	-
$[VO(L^4)]$ **4**	3277	1648	1468	1237	967

H_2L^5	-	1582	1484	1226	-
[Cu(HL^5)] **8**	-	1641	1485	1244	-
H_2L^6	-	1728	1480	1226	-
[VO(L^6)] **5**	-	1644	1473	1237	953
[Cu(HL^6)] **9**	-	1632	1488	1222	-

EPR. All complexes were characterized by X-band electron paramagnetic resonance (EPR) spectroscopy to get further structural insight. Spectra were measured in MeOH and simulated[12] to determine the spin Hamiltonian parameters, which are included in **Table S4**. **Figure S2** depicts the spectra measured at *ca.* 100 K.

While all Cu(II) complexes show similar z-component hyperfine coupling parameters, for the vanadium complexes differences are found. Complexes **1** and **2** in MeOH display features corresponding to the presence of at least two distinct $V^{IV}O$-species, while complexes **3**-**5** show only one. Moreover, the species which presents the lower hyperfine coupling parameters ($|A_z|$) in the spectra of **1** and **2** seems to correspond to the same type of species found in solutions of complexes **3**-**5** (see **Fig. S3**). For the oxidovanadium(IV) complexes the coordination in the equatorial 'plane' can be predicted through the $|A_z|_{calc}$ values, by applying the additivity relationship initially developed by Wüthrich[13] and Chasteen.[14] An $|A_z|_{calc}$ value of 167.1×10^{-4} cm^{-1} is obtained considering an equatorial coordination involving ($O_{phenolate}$, N_{amine}, $O_{carboxylate}$, MeOH),[15, 16] which fits well the experimental parameters determined for **3**-**5**. Additionally, the spin Hamiltonian parameters measured for **5** in MeOH are in good agreement with those found in THF and previously reported: g_z = 1.938 and $|A_z| = 168.2\times10^{-4}$ cm^{-1}.[1] As described in that report, the assignment of the binding mode is not straightforward as different sets of donor groups result in $|A_z|_{calc}$ values which are within the accepted error ($\pm3\times10^{-4}$ cm^{-1}),[13-15] however, the similarity of the parameters obtained for the complexes with (**5**) or without the tripodal 2MePy moiety (*p.e.* **3** and **4**), support the suggested equatorial binding mode: $O_{phenolate}$, N_{amine}, $O_{carboxylate}$ and a solvent molecule. The $|A_z|$ value determined for the second species in the EPR spectrum of complex **2** agrees with having the $O_{phenolate}$

occupying the axial position and a second molecule of solvent completing the equatorial plane ($|A_z|_{calc}$ = 174.2×10^{-4} cm^{-1}).

Table S4 – Spin Hamiltonian parameters obtained from the frozen MeOH solution EPR spectra of the complexes measured at *ca.* 100 K.

Compound	$g_{x,y}$	g_z	$\|A_{x,y}\|$×10^4 cm^{-1}	$\|A_z\|$×10^4 cm^{-1}	$g_z/\|A_z\|$
VO(L^1) (**1**)	1.985	1.953	60.4	169.6	
	1.985	1.940	60.0	179.3	
VO(L^2) (**2**)	1.979	1.942	63.5	172.6	
	1.985*	1940*	60.0*	179.3*	
VO(L^3) (**3**)	1.978	1.947	59.6	167.0	
VO(L^4) (**4**)	1.979	1.949	57.9	165.7	
VO(L^6) (**5**)	1.979	1.942	60.6	167.5	
Cu(L^1) (**6**)	2.051	2.279	17.0	172.6	132.1
Cu(L^3) (**7**)	2.052	2.280	18.0	170.9	133.4
Cu(L^5) (**8**)	2.067	2.270	31.5	171.6	132.3
Cu(L^6) (**9**)	2.070	2.273	30.0	173.2	131.2

* values included are the same as obtained for **1**, as this species amount is too low to be simulated.

For all Cu(II) complexes $g_z > g_{x,y} > 2.0$, indicating the presence of a $d_{x^2-y^2}$ ground state in copper(II) located in tetragonally elongated pseudo-octahedral, square-planar or square-based pyramidal geometries.[17] The spin Hamiltonian parameters obtained for these Cu(II) complexes correlate well with those obtained by G. Tabbì *et al.*[18] for Cu-complexes with N,O as donor atoms. Related Cu-complexes containing either COO^- or $N_{pyridinic}$ instead of $O_{phenolate}$ were reported by some of us[19, 20] and the determined spin Hamiltonian parameters are included in **Fig. S4**, showing only a decrease in g_z when going from COO^- to $N_{pyridinic}$ coordination, the $|A_z|$ values being quite similar. In complexes **8** and **9** coordination in solution could involve the pyridinic N atom from the 2MePy, as in the solid state, however, the similarity of the spin Hamiltonian parameters obtained for complexes **6**, **7** with complexes **8**, **9**, does not support its coordination, at least in the equatorial plane,

towards which the d_{x2-y2} orbital points its lobes. Moreover, no superhyperfine coupling was found in the EPR spectra of complexes **8** and **9**, which was found in the spectra of the related pyridinic derivatives.[19] Therefore we propose a similar binding mode for all Cu(II)-complexes in MeOH. The high values observed for the tetrahedral distortion index $g_z/|A_z|$ suggests the presence of small distortions in square based geometries.[21]

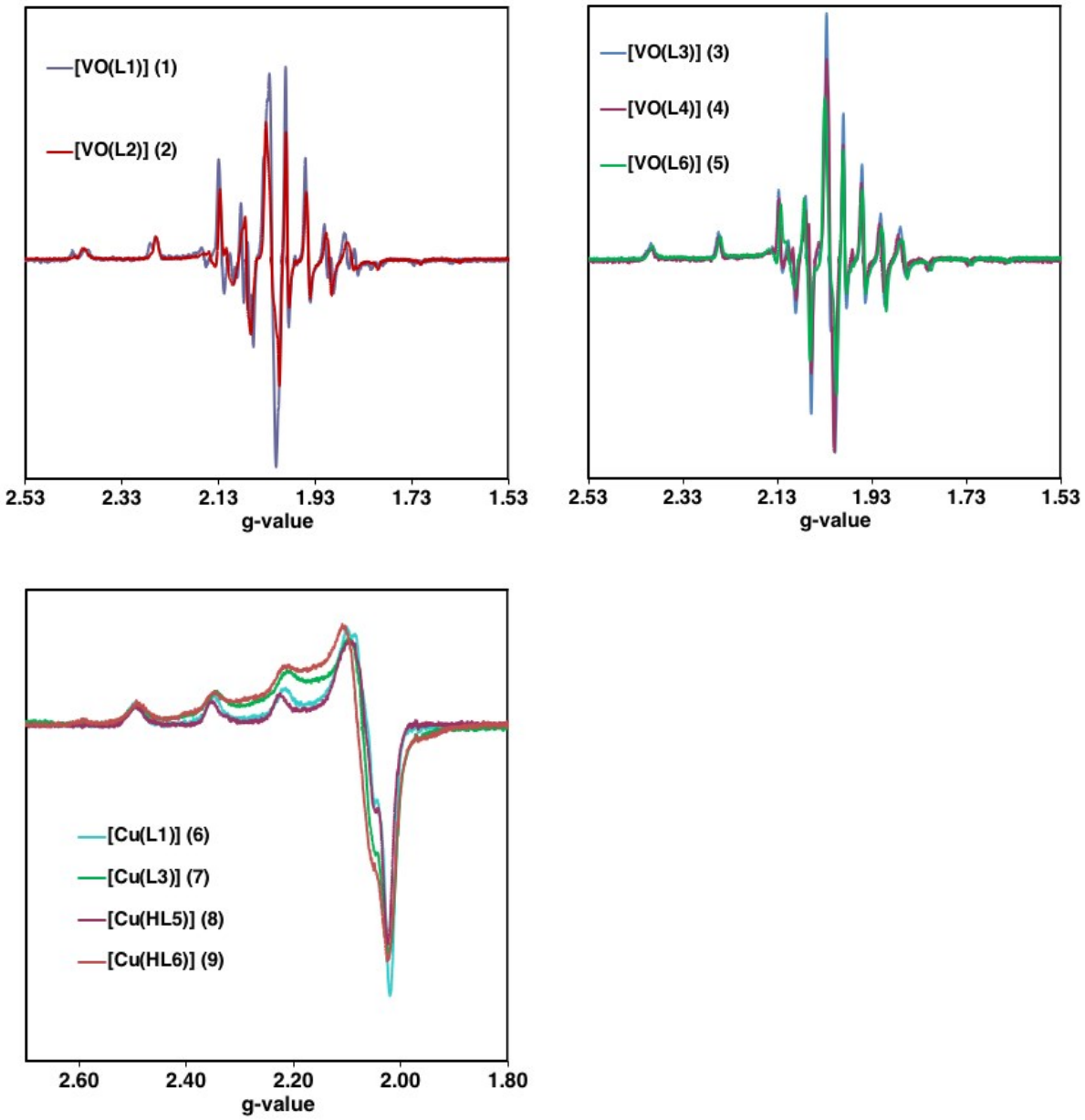

Figure S2 – First derivative X-Band EPR spectra measured in MeOH at *ca.* 100K. The concentration of complexes was in the range 1-3 mM.

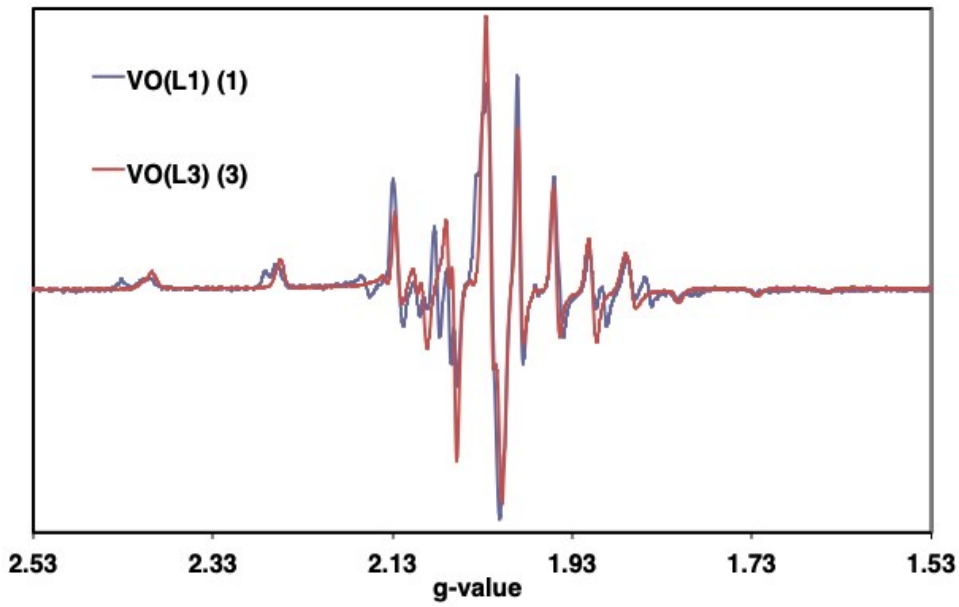

Figure S3 – X-Band EPR spectra measured in MeOH at ca. 100 K for complexes [VO(L^1)] **1** and [VO(L^3)] **3**, showing that the $V^{IV}O$-species with the lower $|A_z|$ value for **1** (inner) has similar parameters to the only $V^{IV}O$-species found for **3**.

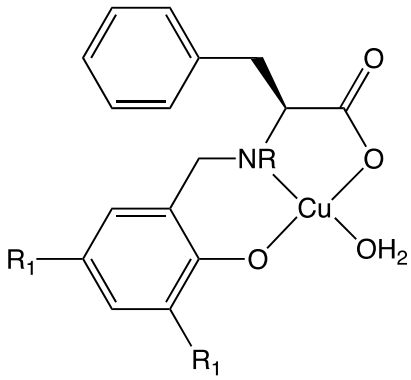

Solvent: MeOH
g_z = 2.27-2.28
$|A_z|$ = 170.9-173.2 x10^{-4} cm^{-1}
d-d band = 675-698 nm
This work

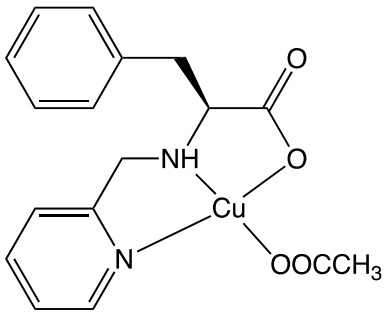

Solvent: Ethyleneglycol
g_z = 2.26
$|A_z|$ = 181 x10^{-4} cm^{-1}
d-d band ~ 670 nm
P. Adão et al. 2015

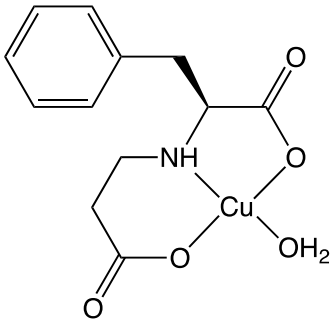

Solvent: DMSO
g_z ~ 2.29
$|A_z|$ = 181.5 x10^{-4} cm^{-1}
d-d band = 700-710 nm
P. Adão et al. 2019

Figure S4 – General formula and spin Hamiltonian and UV-Vis absorption parameters obtained in this work and for related Cu-complexes: P. Adão et al. 2015[19] and P. Adão et al. 2019[20].

UV-Vis absorption and circular dichroism spectroscopy- All ligand precursors show strong bands in the UV range due to $\pi-\pi^*$ transitions in the aromatic rings (**Fig. S6**). The presence of the 2MePy side arm in H_2L^5-H_2L^6 results in more intense bands in the 250-280 nm range. In general, these intraligand bands in the UV range appear with higher intensity in the spectra of the complexes. All Cu(II)-complexes show one band (or an envelope of bands) between 650-700 nm, due to d–d transitions,[22, 23] in agreement with a d_{x2-y2} ground state and similar to those observed for related complexes.[19, 20] However, it is possible to verify that in [Cu(HL^5)] (**8**) and [Cu(HL^6)] (**9**) the d-d band is red-shifted by *ca.* 27 nm when compared to bands in complexes [Cu(L^1)] (**6**) and [Cu(L^3)] (**7**), suggesting a slightly weaker ligand field, possibly arising from the coordination of N_{pyr} pendant arm and a chlorido ligand in equatorial positions of a square-pyramidal Cu(II) centre.[18] Ionochromism has been reported for related Cu(II) complexes, where the respective absorption maxima have been reported to be dependent on ligand-field strength.[24-28] Furthermore, [Cu(L^1)] (**6**) and [Cu(L^3)] (**7**) present absorption bands at 430 and 440 nm, respectively, which are assigned to ligand to metal phenolate→Cu(II) charge transfer transitions.[29, 30] The pattern of the CD spectra of [Cu(HL^5)] (**8**) and [Cu(HL^6)] (**9**) in MeOH (**Fig. S7**) is the same in the UV-vis range, as well as their intensity in the visible range. This indicates that the coordination geometry is the same. In the corresponding absorption spectra (**Fig. S6**), complex [Cu(HL^5)] presents a much weaker band at 466 nm, while [Cu(HL^6)] has no bands in this region. These might be due to the protonatonation of the phenol donor, decreasing its ability to donate electronic charge to the Cu center. The SC-XRD structure of complex [Cu(HL^6)] (**9**) showed the phenol coordinated to Cu in the protonated form, and these spectroscopic data suggests the same happens in MeOH solution.

The spectra of oxidovanadium(IV) complexes [VO(L^1)] and [VO(L^2)] are very similar and no d-d bands are clearly distinguished as they are probably under the tail of strong ligand to metal charge transfer (LMCT) bands at *ca.* 350 nm. The bands appearing as shoulders at ~ 500 nm are probably also LMCT bands, due to oxidation of the V-center. [VO(L^3)] and [VO(L^4)] (**Fig. S6**) show at least two bands at different

energies that probably have contributions but are too intense to be solely due to d-d transitions.

The V-complex with the ligand containing the tripodal amine, [VO(L^6)] (**5**), was reported to oxidize very fast[1] and the very strong LMCT band centered at 565 nm was assigned to a $O_{phenolate} \rightarrow V^V$ $p\pi$-$d\pi^*$ transition, typical of phenolate-bound V^VO^{3+} species.[31] However, we studied the oxidation process of [VO(L^3)] and [VO(L^6)] in MeOH:PBS buffer (1:1 v/v) and while [VO(L^3)] easily oxidizes in solution (see section 2.2.2), [VO(L^6)] showed very high stability in mM concentration, showing no signs of oxidation. We did however, realize that the spectra of [VO(L^6)] in the Vis range changes drastically with pH (see **Fig. S5**) and at pH> 7 the band that was observed in MeOH at 565 nm, shifts to 595 nm in MeOH: H2O, and is blue shifted to 400 nm in this solvent upon increasing the pH. This can perhaps be explained by the protonation (lower pH) / deprotonation (higher pH) of the phenol group, that shifts the LMCT band from lower to higher energy as deprotonation occurs.

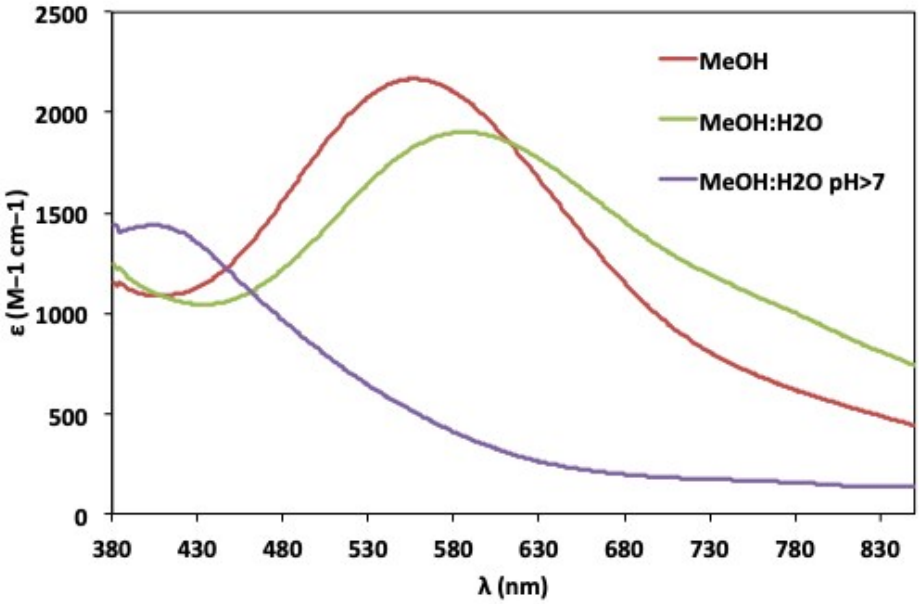

Figure S5 – UV-vis absorption spectra of [VO(L^6)] (**5**) in several media: MeOH, MeOH:H_2O (1:1) and MeOH:H_2O (1:1) at pH > 7 (a few drops of NaOH were added). [**5**] ~0.4 mM.

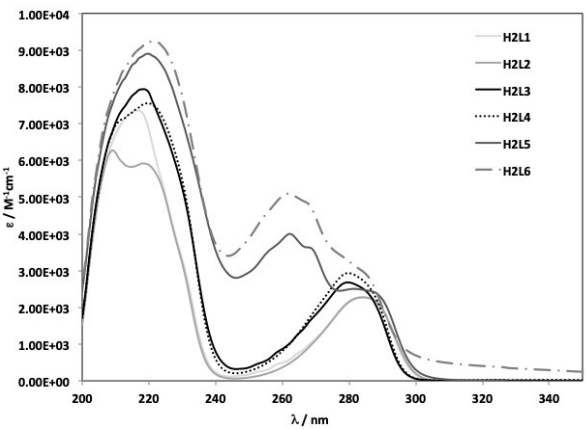

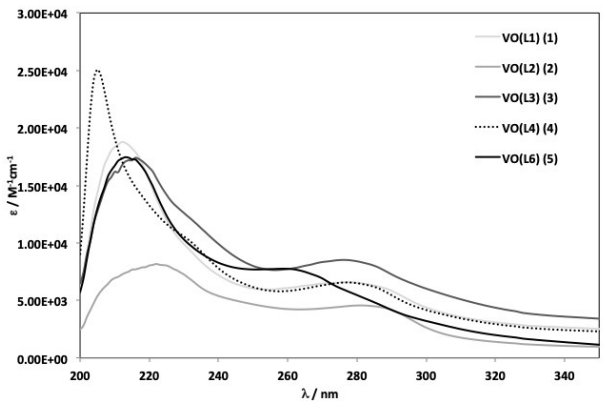

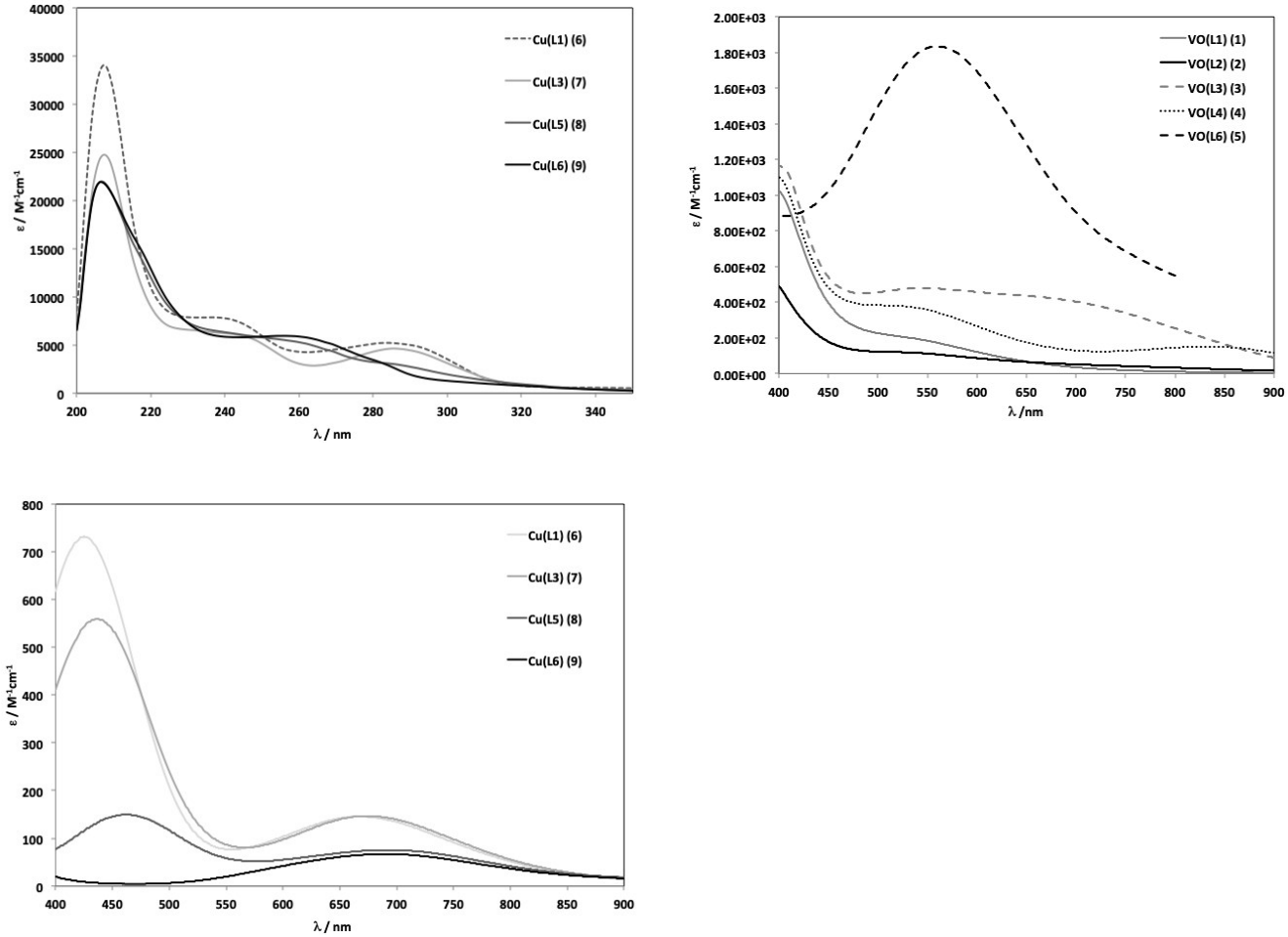

Figure S6 – UV-Vis absorption spectra of ligand precursors and complexes in MeOH. Optical path = 1.0 cm. [Ligands] = 2.5×10^{-4} M. Complex concentrations in the UV range 1-5×10^{-4} M and in the Vis range 1-3 $\times10^{-3}$ M.

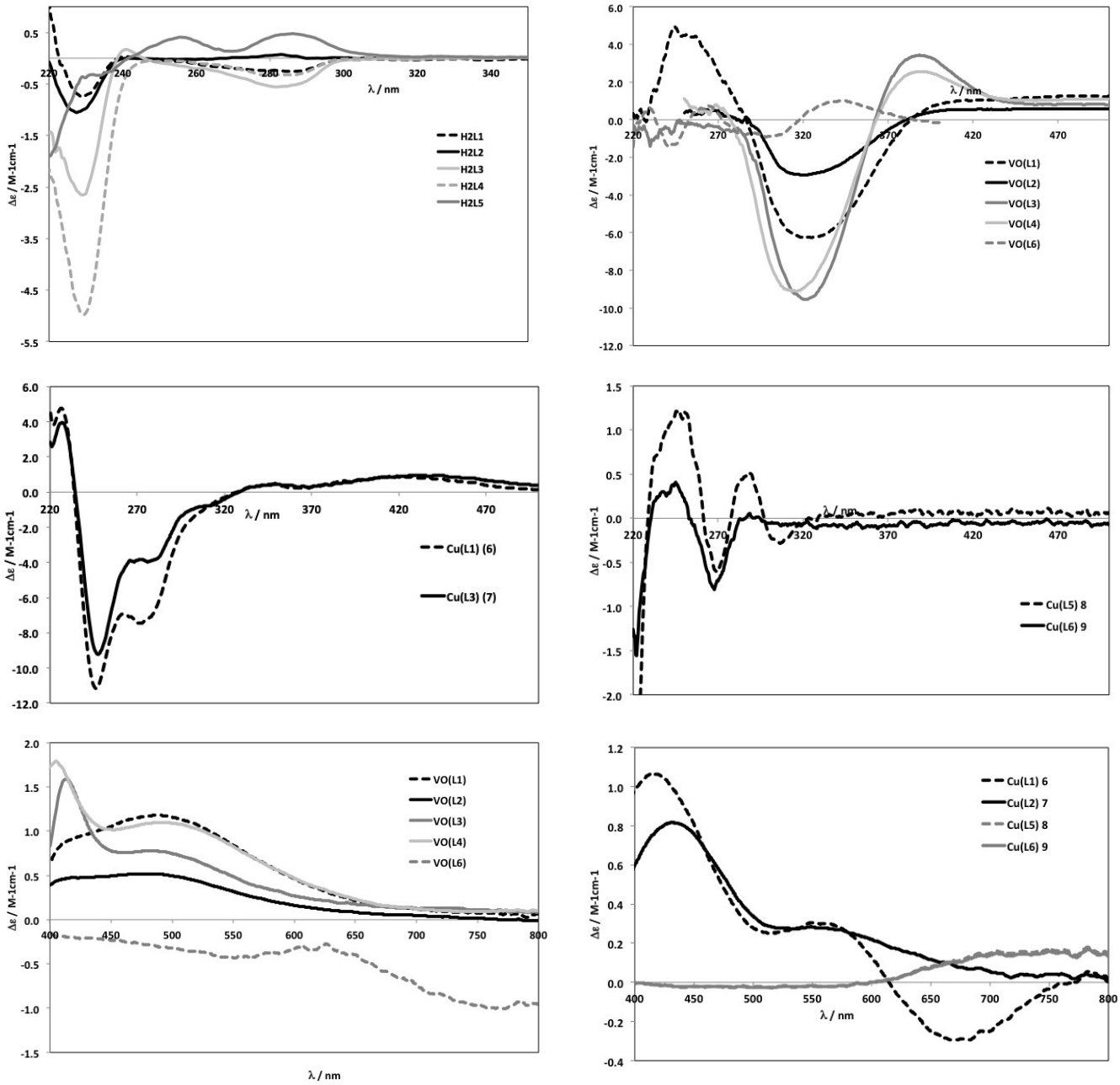

Figure S7 – Circular dichroism spectra in the UV and Vis range of ligand precursors and complexes in MeOH. [Ligands] = 2.5×10^{-4} M, optical path 1.0 cm. Complex concentrations: in the UV range $1\text{-}5\times10^{-4}$ M and optical path 1.0 cm and in the Vis range $1\text{-}3\times10^{-3}$ M and optical path 2.0 mm.

S2 – Stability

Vanadium complexes are known to oxidize easily in solutions under air. In order to study the oxidation process complexes [VO(L^3)] (**3**) and [VO(L^6)] (**5**) were selected, since they are the V-complexes that showed the most relevant results in cell-based studies. EPR and NMR studies were done (see **Fig. S8-S10**). Regarding the assignment of the ^{51}V NMR peaks, the question is whether they correspond to V^V-complexes containing the ligand or oligomeric inorganic vanadate species. The speciation of vanadium(V) in aqueous environments has been studied, and the ^{51}V NMR chemical shift of species with different nuclearities, charge and protonation states, depends among other things, on the pH.[32-34] Monovanadate (V_1) at pH 7.4 resonates between −555 and −560 ppm, but it is present as a sharp peak, not a broad band as observed in the spectra of complex [VO(L^3)]. Moreover, if the oxidation yielded free ligand additional peaks should have been observed in the proton NMR, for free and coordinated ligand, however only a set of peaks is present in the ^1H NMR spectra. Therefore, we can assume that the species observed after oxidation of complex [VO(L^3)] (δ_V = −520.6 ppm) is a V(V)-complex containing the ligand in its coordination sphere.

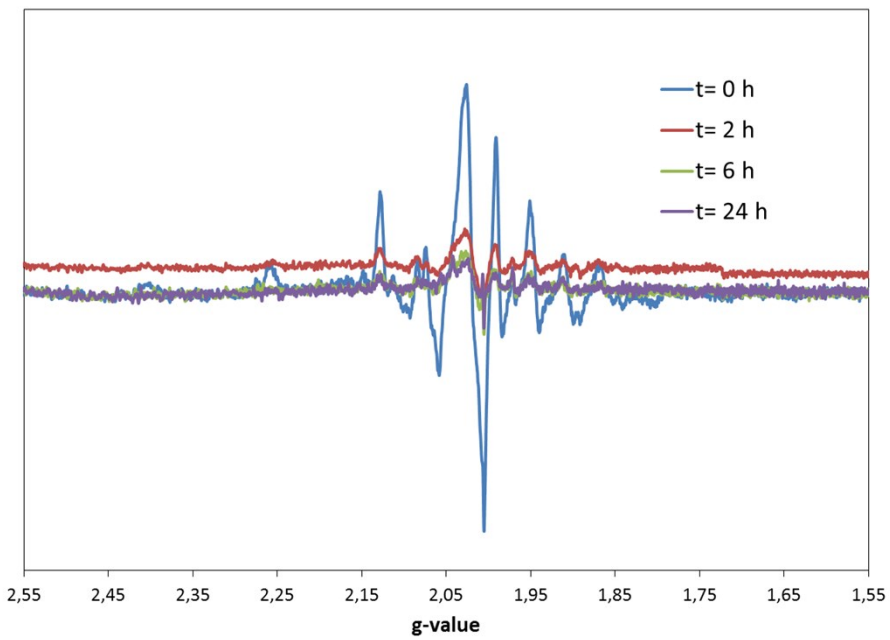

Figure S8 – X-band EPR spectra of a 2.5 mM solution of **3** [VO(L^3)] in MeOH:H_2O 1:1 (v/v) (pH 4.5), which were frozen in liquid nitrogen after 0, 2, 6 and 24 h of dissolution.

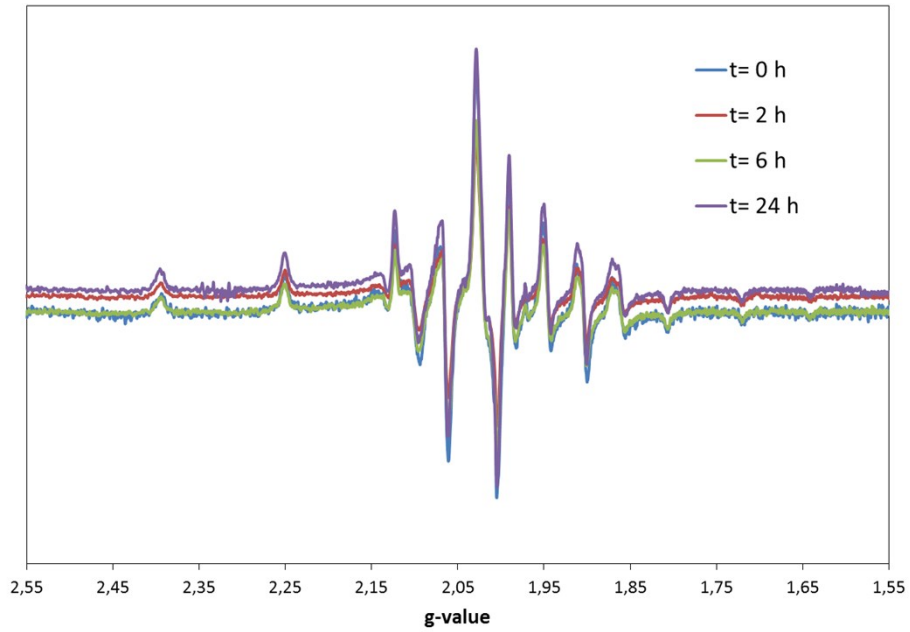

Figure S9 – X-band EPR spectra of a 2.5 mM solution of **5** [VO(L^6)] in MeOH:H_2O 1:1 (v/v) (pH 6.9), which were frozen in liquid nitrogen after 0, 2, 6 and 24 h of dissolution.

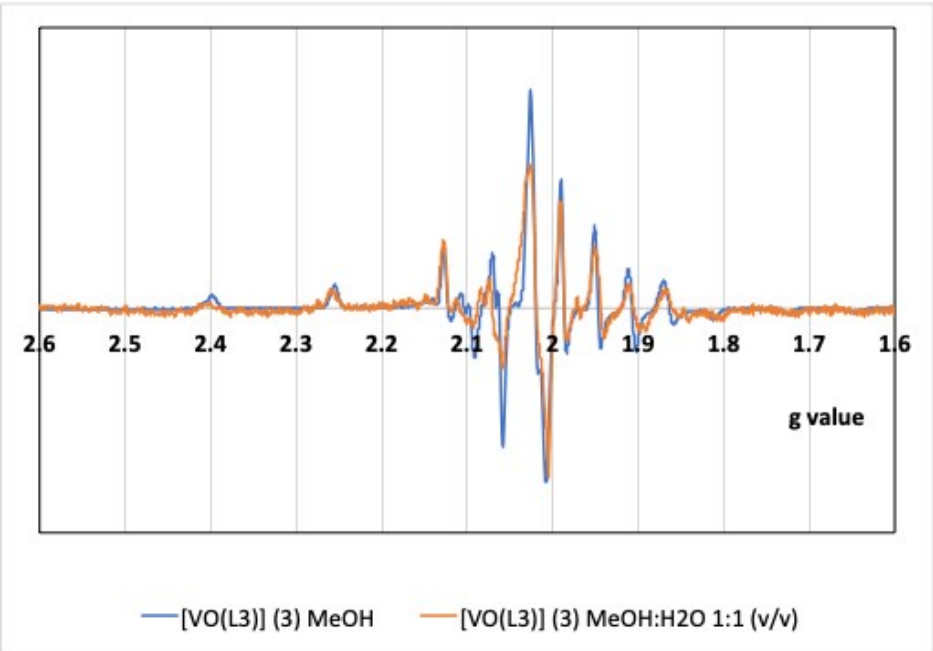

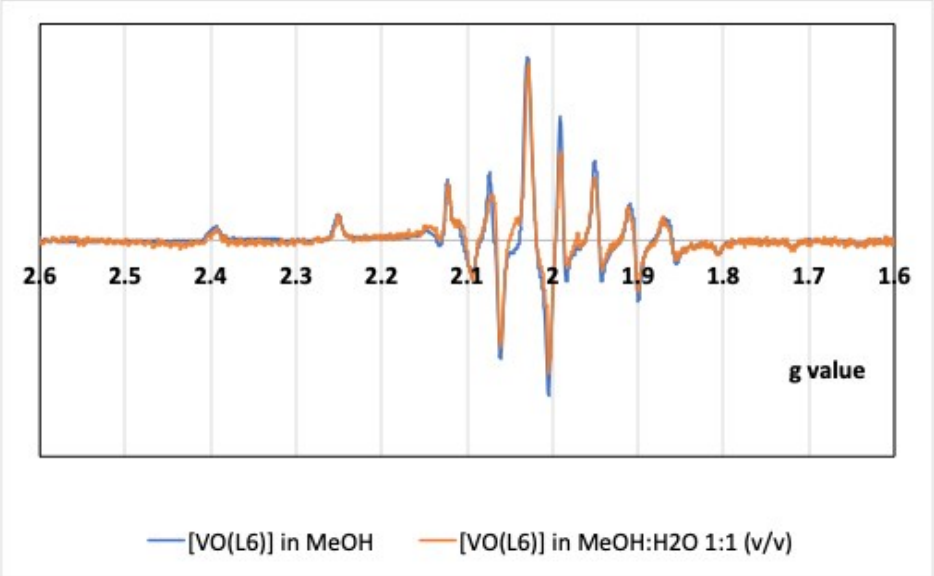

Figure S10 – X-band EPR spectra of [VO(L^3)] and [VO(L^6)] in MeOH:H_2O 1:1 (v/v) (pH 6.9) and in MeOH.

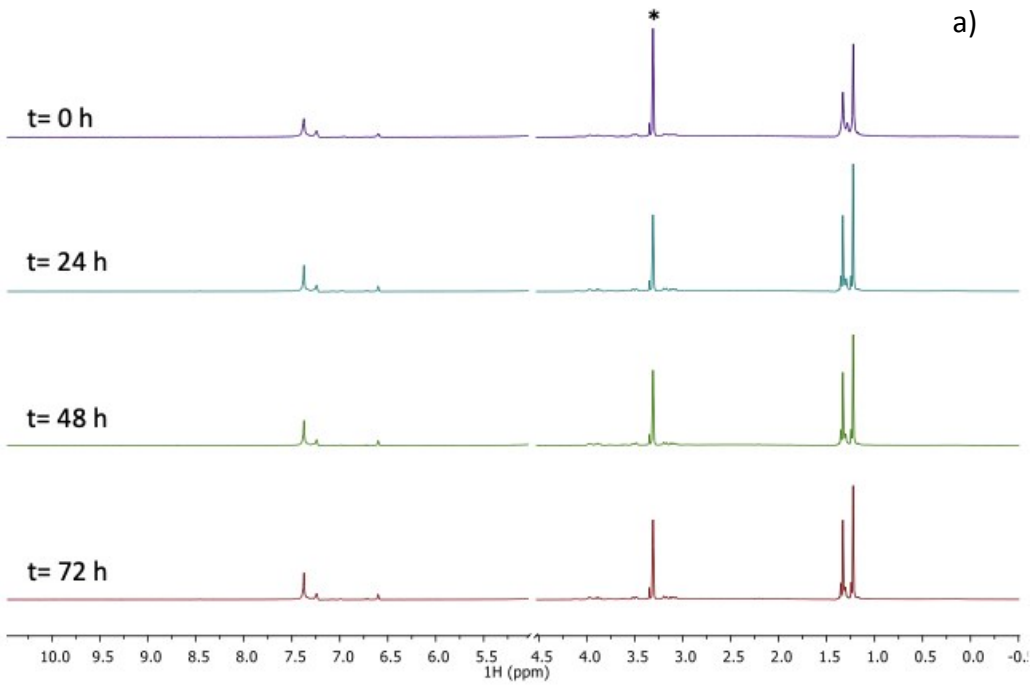

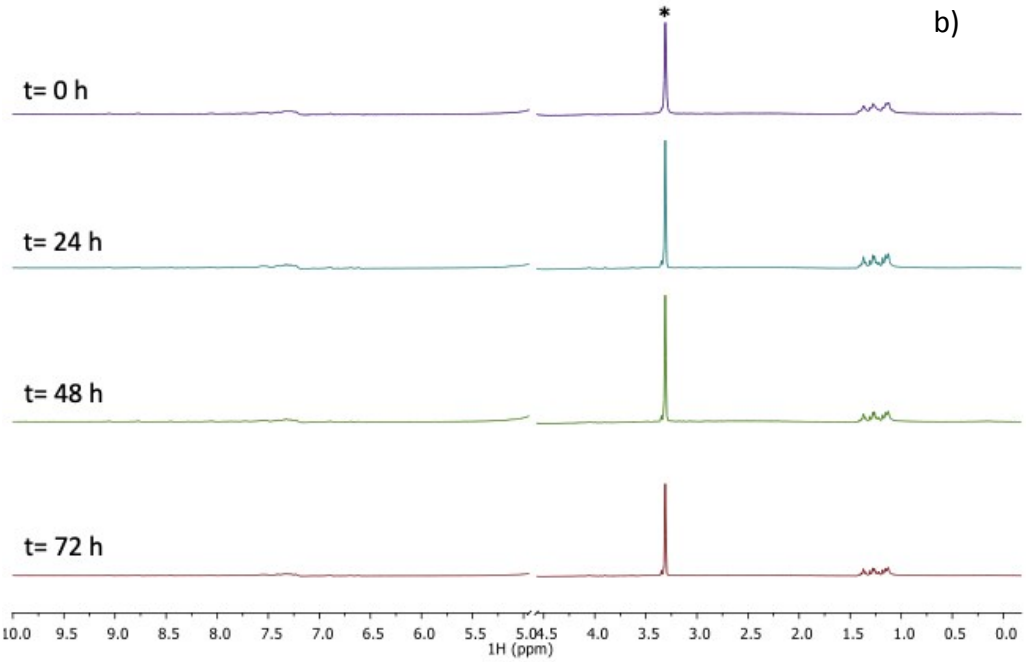

Figure S11 - ^{1}H NMR spectra of 3.5 mM solutions of **3** [VO(L^3)] (a) and **5** [VO(L^6)] (b) in in CD_3OD:PBSaq 1:1 (v/v) (pH *ca.* 7.4) measured at different time points indicated in the legend. The ^{1}H NMR spectrum at t = 0 h in a) is multiplied by 30 to be comparable with the other spectra.* corresponds to the MeOH signal.

S3 – DNA binding

Materials and Methods

Calf thymus DNA (ct-DNA) and phosphate buffer saline (PBS, as readily soluble tablets) were purchased from Sigma-Aldrich. Methanol spectroscopic grade from Carlo Erba was used to prepare the complexes' stock solutions. Doubly distilled deionized water was used throughout.

The stock solution of DNA was prepared in PBS and its purity was verified by monitoring the ratio of absorbance at 260 nm to that at 280 nm, which was 1.88, indicating that the DNA was sufficiently free of protein. The concentration 2.99×10^{-3} $Mnuc^{-1}$ was determined by the intensity of UV spectrum at 260 nm with a molar extinction coefficient value of 6600 $M^{-1}cm^{-1}$.

UV-Visible spectra were recorded using a Perkin Elmer Lambda 35 spectrophotometer in the range 200-700 nm. The reference solution was the corresponding PBS solution. Equal amounts of DNA were added to the sample and reference cuvette to eliminate the absorbance of DNA itself, keeping the concentration of the complex and increasing the concentration of DNA. The solutions were equilibrated for 5 minutes before running the spectrum in a 1 cm path length cuvette.

Figure S11 shows the changes observed in the UV-Vis spectra upon titrating the compounds with increasing amounts of DNA and the insets the fitting which was made with a least squares model described in [35]. **Table S5** includes the constants determined.

Table S5 – Conditional binding constants obtained from the UV-Vis absorption titrations, using a least square fit described in [35].

Compound	H_2L^3	H_2L^5	$[VO(L^3)]$ (**3**)	$[Cu(L^3)]$ (**7**)	$[Cu(HL^5)]$ (**8**)
K_b / M^{-1}	5.96×10^1	2.28×10^3	3.27×10^3	2.66×10^3	1.96×10^3

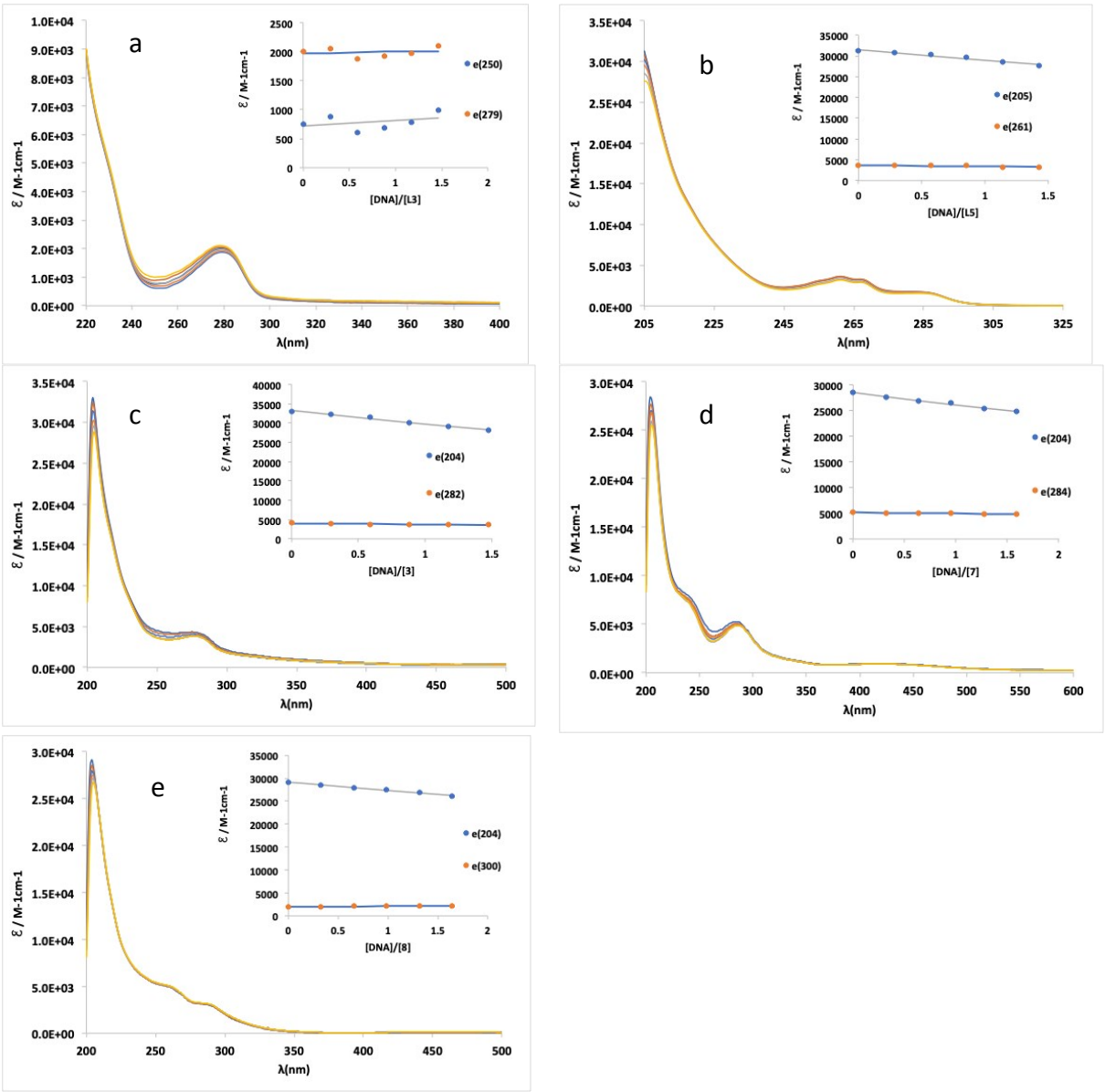

Figure S12– UV-vis spectra measured for the titration of a) H_2L^3, b) H_2L^5, c) [VO(L^3)] (**3**), d) [Cu(L^3)] (**7**) and e) [Cu(HL^5)] (**8**) with increasing amounts of calf thymus DNA. The [DNA]:[compound] ratios are indicated in the x axis of the inset. The initial concentrations are the following: [H_2L^3] = 4.26×10^{-5} M, [H_2L^5] = 4.36×10^{-5} M, [**3**] = 4.23×10^{-5} M, [**7**] = 3.91×10^{-5} M and [**8**] = 3.79×10^{-5} M. Insets show the variation of the molar absorptivity at two wavelengths with the [DNA]:[compound] ratio; the lines show the fitted model to determine the binding constants of the compounds with DNA using a least squares fit described in [35].

S4 – Cytotoxicity data

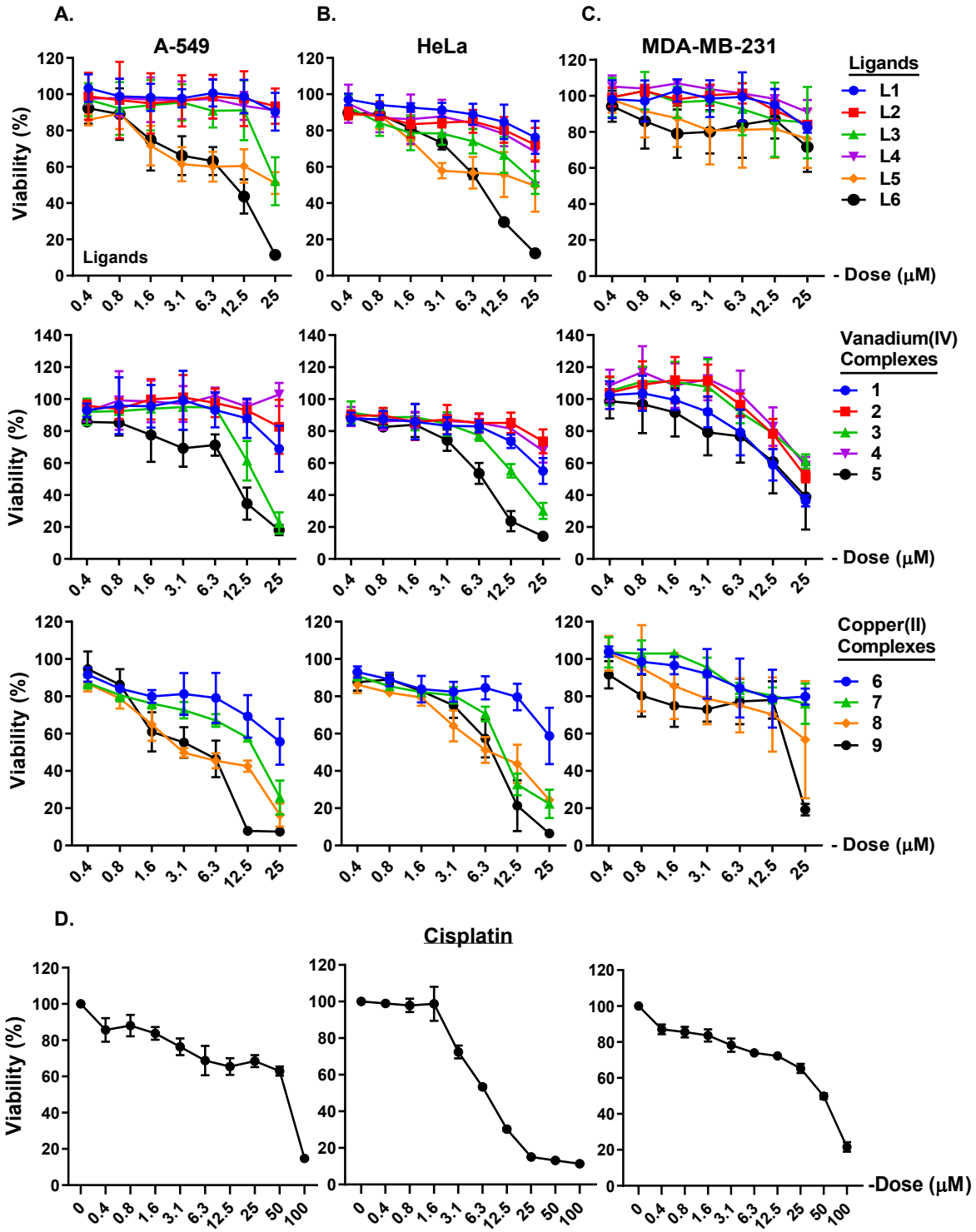

Figure S13 – Cell viability curves of A-549 (**A**), HeLa (**B**) and MDA-MB-231 (**C**) cells in response to the ligand precursors (H_2L^1 - H_2L^6) and their corresponding metal complexes (vanadium, **1-5**; copper **6-9**) following incubation for 72 h. Cell viability curves of the three

cell lines incubation with positive control Cisplatin for 72h (**D**). Cell viability was measured using the MTT assay and normalized to untreated cells. Lines represent mean ± SD (n=3).

References

[1] C.M. Teixeira, P. Adao, M.F.N.N. Carvalho, C.S.B. Gomes, J.C. Pessoa, Inorg. Chim. Acta, 510 (2020) 119727.
[2] F.F. Blicke, Org. React., 1 (1942) 303.
[3] A. John, M.M. Shaikh, P. Ghosh, Dalton Trans., (2008) 2815-2824.
[4] N. Berthet, V. Martel-Frachet, F. Michel, C. Philouze, S. Hamman, X. Ronot, F. Thomas, , Dalton Trans., 42 (2013) 8468-8483.
[5] H. Saimiya, Y. Sunatsuki, M. Kojima, S. Kashino, T. Kambe, M. Hirotsu, H. Akashi, K. Nakajima, T. Tokii, Dalton Trans., (2002) 3737-3742.
[6] Z.D. Matović, G. Pelosi, S. Ianelli, G. Ponticelli, D.D. Radanović, D.J. Radanović, Inorg. Chim. Acta, 268 (1998) 221-230.
[7] A.W. Addison, T.N. Rao, J. Reedijk, J. van Rijn, G.C. Verschoor, J. Chem. Soc., Dalton Trans., (1984) 1349-1356.
[8] G.B. Deacon, R.J. Phillips, Coord. Chem. Rev., 33 (1980) 227-250.
[9] K. Nakamoto, Infrared and Raman Spectra of Inorganic and Coordination Compounds: Part A: Theory and Applications in Inorganic Chemistry, Sixth Edition, 5th ed., Wiley, 2008.
[10] J.C. Pessoa, M.J. Calhorda, I. Cavaco, I. Correia, M.T. Duarte, V. Felix, R.T. Henriques, M.F.M. Piedade, I. Tomaz, J. Chem. Soc. Dalton Trans., (2002) 4407-4415.
[11] L. Vilas Boas, J. Costa Pessoa, Vanadium, in: G. Wilkinson, R.D. Gillard, J.A. McCleverty (Eds.) Comprehensive Coordination Chemistry, Pergamon, Oxford, 1987, pp. 453-583.
[12] A. Rockenbauer, L. Korecz, Appl. Magn. Reson., 10 (1996) 29-43.
[13] K. Wuthrich, Helv. Chim. Acta, 48 (1965) 1012-1017.
[14] N.D. Chasteen, Biological Magnetic Resonance, Plenum, New York, 1981.
[15] T.S. Smith, R. LoBrutto, V.L. Pecoraro, Coord. Chem. Rev., 228 (2002) 1-18.
[16] J.C. Pessoa, I. Correia, T. Kiss, T. Jakusch, M.M.C.A. Castro, C.F.G.C. Geraldes, J. Chem. Soc. Dalton Trans., (2002) 4440-4450.
[17] E. Garribba, G. Micera, J. Chem. Edu., 83 (2006) 1229.
[18] G. Tabbi, A. Giuffrida, R.P. Bonomo, J. Inorg. Biochem., 128 (2013) 137-145.
[19] P. Adao, S. Barroso, M.F.N.N. Carvalho, C.M. Teixeira, M.L. Kuznetsov, J.C. Pessoa, Dalton Trans., 44 (2015) 1612-1626.
[20] P. Adão, C.M. Teixeira, M.F.N.N. Carvalho, M.L. Kuznetsov, C.S.B. Gomes, J.C. Pessoa, Mol. Catal., 475 (2019) 110480.
[21] U. Sakaguchi, A.W. Addison, J. Chem. Soc. Dalton Trans., (1979) 600-608.
[22] S. Keinan, D. Avnir, J. Chem. Soc. Dalton Trans., (2001) 941-947.
[23] R.C. Pratt, C.T. Lyons, E.C. Wasinger, T.D. Stack, J. Am. Chem. Soc., 134 (2012) 7367-7377.
[24] Y.-H. Zhou, J. Tao, Q.-C. Lv, W.-G. Jia, R.-R. Yun, Y. Cheng, Inorg. Chim. Acta, 426 (2015) 211-220.

[25] E. Safaei, H. Bahrami, A. Wojtczak, S. Alavi, Z. Jagličić, Polyhedron, 122 (2017) 219-227.
[26] S.A. Haque, R.L. Bolhofner, B.M. Wong, M.A. Hossain, RSC Adv., 5 (2015) 38733-38741.
[27] J.S. Mendy, M.A. Saeed, F.R. Fronczek, D.R. Powell, M.A. Hossain, Inorg. Chem., 49 (2010) 7223-7225.
[28] L. Rostami, H. Golchoubian, Inorg. Chim. Acta, 462 (2017) 215-222.
[29] G. Zhan, W. Zhong, Z. Wei, Z. Liu, X. Liu, Dalton Trans., 46 (2017) 8286-8297.
[30] V. Kumar, S. Ghosh, A.K. Saini, S.M. Mobin, B. Mondal, Dalton Trans., 44 (2015) 19909-19917.
[31] A. Neves, A.S. Ceccatto, C. Erasmus-Buhr, S. Gehring, W. Haase, H. Paulus, O.R. Nascimento, A.A. Batista, J. Chem. Soc. Chem. Commun., (1993) 1782-1784.
[32] L. Pettersson, B. Hedman, I. Andersson, N. Ingri, Chim. Scripta, 22 (1983) 254-264.
[33] E. Heath, O.W. Howarth, J. Chem. Soc. Dalton Trans., (1981) 1105-1110.
[34] C. Slebodnick, V.L. Pecoraro, Inorg. Chim. Acta, 283 (1998) 37-43.
[35] M.P.C. Campello, E. Palma, I. Correia, P.M.R. Paulo, A. Matos, J. Rino, J. Coimbra, J.C. Pessoa, D. Gambino, A. Paulo, F. Marques, Dalton Trans., 48 (2019) 4611-4624.